Int J Clin Exp Med 2016;9(11):21280-21287
www.ijcem.com /ISSN:1940-5901/IJCEM0020506

Original Article

miR-146 promotes apoptosis of Jurcat cell in children with acute lymphoblastic leukemia by targeting STAT1 expression

Xia Feng*, Jihong Xue*, Kunxia Xie

*Department of Pediatrics, Yan'an University Affiliated Hospital, Yan'an 716000, Shaanxi, China. *Equal contributors and co-first authors.*

Received November 25, 2015; Accepted April 13, 2016; Epub November 15, 2016; Published November 30, 2016

Abstract: Objective: Through detecting miR-146a expression in bone marrow and peripheral blood in children with acute T lymphoblastic leukemia cells (T-ALL), this study aims to investigate the function of miR-146a in Jurkat cells. Methods: QRT-PCR method was used to detect miR-146a expression in bone marrow and peripheral blood of children with acute T-ALL. MiR-146a was transfected into Jurkat cells by lipofection method. CCK-8 assay and flow cytometry method were used to detect the influences of miR-146a on proliferation and apoptosis of Jurkat cells. Western blot was used to detect the expression of signal transducer and activator of transcription 1 (STAT1) gene. After inference of STAT1 expression *in vitro*, the changes of proliferation, apoptosis of Jurkat cells were detected. The dual luciferase assay was used to identify whether miR-146a can directly target STAT1 gene. Results: Compared with the control group, miR-146a expression was significantly decreased in bone marrow and peripheral blood in T-ALL. When compared with the middle-risk group, miR-146a expression was decreased in bone marrow and peripheral blood in high-risk group. After transfection of miR-146a mimics *in vitro*, the proliferation of Jurkat cells was decreased significantly and the apoptosis rate was increased significantly, and STAT1 protein expression was also down-regulated. After interference of STAT1 protein expression, the proliferation of Jurkat cells was inhibited and the apoptosis rate was increased. It was shown by dual luciferase assay that miR-146a can directly combine with STAT1. Conclusion: MiR-146 expression is decreased in bone marrow and peripheral blood in Children with T-ALL, which is associated with the development of T-ALL. *In vitro*, miR-146a can repress Jurkat cell proliferation and promote cell apoptosis, which may be a potential target for treatment of T-ALL in the future.

Keywords: MiR-146a, acute lymphoblastic leukemia, STAT1

Introduction

Acute T Lymphoblastic Leukemia (T-ALL) is one of the most common hematologic malignances in clinic [1], and it originates from the thymus and accounts for about 15% of children with ALL, which become a serious threat to health of children [2]. The main clinical manifestations of T-ALL are diffuse infiltration of immature T lymphocytes in bone marrow, leukocyte increasing, Mediastinal lymph node enlargement and central nervous system involvement [3]. In recent years, the complete cure rate of T-ALL is increase to a certain extent as the improvement of combined chemotherapy, which reached to 70% for children patients [4]. But when it is compared with B-lymphocytic leukemia, the prognosis is still poor. Exploring new treatment is still necessary. Currently, the morbidity and progression of T-ALL is reported to be associated with proliferation, differentiation, apoptosis and other abnormal behaviors [5], but the mechanisms are still unclear. Therefore, it is important and valuable to explore new therapeutic targets of T-ALL.

MiRNA is a class of small non-coding RNA with length about 18-25 nt, which broadly participate different physiological and pathological processes through binding to 3'-UTR of target genes [6, 7]. MiRNA plays as an important regulator to inhibit mRNA translation or degrade target mRNA [8]. Studies have shown that miRNA can play as oncogenes or tumor suppressor genes to influence tumor proliferation, invasion, metastasis and resistance to chemotherapy

[9]. Frezzetti et al. found that miR-21 can regulate oncogene Ras to influence the proliferation of thyroid cancer cells [10]. Tavazoie et al. demonstrated that miR-335 and miR-126 played as tumor suppressor gene in breast cancer, in which the down-regulated miRNAs promoted the development of breast cancer [11]. Identification of tumor-associated miRNAs can provide a new therapeutic way for the clinical treatment of cancers. This study aimed to explore the role of miR-146a in children with T-ALL, which presents new biomarkers in the diagnosis and treatment of T-ALL.

Materials and methods

Sample collection

This study included 54 children patients of T-ALL from October 2007 to July 2014 in Yanan University Affiliated Hospital, which included 34 males and 20 females with average age of 9.5 years old. All children were confirmed by morphology of bone marrow, cytochemistry, and immunological analysis. Based on diagnosis standard, all children patients were classified into high-risk group (36 cases) and middle-risk group (18 cases). The bone marrow fluid and peripheral blood were collected for each patient. The bone marrow fluid and peripheral blood were collected from 15 children patients for bone orthopaedic surgery, who were confirmed without any tumor or blood diseases as normal control group. Prior written and informed consent were obtained from every patient and the study was approved by the ethics review board of Yan'an University Affiliated Hospital.

Cell culture

Jurkat cells were cultured with RPMI-1640 complete medium (Hyclone, Logan, Utah, USA) at 37°C, 5% CO_2 incubator, and HEK293 cells were cultured by DMEM medium (Hyclone, Logan, Utah, USA) with high glucose. When the growth density reaches 80-90%, cells were passaged, and the medium was replaced every two days.

RNA isolation from bone marrow fluid and peripheral blood and qRT-PCR

Total 100 μl bone marrow fluid and 250 μl peripheral blood was thoroughly mixed with 750 μl Trizol (Invitrogen, California, USA) respectively, and the RNA was extracted by phenol-chloroform methods. The RNA quality was checked by gel electrophoresis and the ratio of 260/280 by Spectrophotometer. The miRNA cDNA was reversely transcribed by PolyA tailing method [12] for each 0.5 μg total RNA, and the cDNA was stored in -20°C refrigerator. The reverse transcription of miRNA was followed the procedure: 6 μl RNA template was added to RNase free EP of ice precooling, 2× miRNA Reaction Buffer Mix 10 μl, 0.1% BSA 2 μl, miRNA PrimeScript RT Enzyme Mixture (TaKaRa, Dalian, China) 2 μl, totally 20 μl. The qRT-PCR method was used to detect the expression change of miR-146a by SYBR PrimeScript RT-PCR Kit (TaKaRa, Dalian, China) based on the standard protocol from manufacture.

Transfection of AgomiR-146a into Jurkat cells

The cultured Jurkat cells were divided into two groups, miR-146a mimic group and Negative Control (NC) group. For transfection, cells were cultured in antibiotic-free RPMI-1640 medium with 10% FBS. Total 1.25 μl 20 μM AgomiR-146a and 2 μl Lipo 2000 (Invitrogen, California, USA) was added into EP tubes containing 50 μl Opti Memi medium respectively. The 2 tubes were mixed together after 5 min standing, then followed by another 20 min standing at room temperature. The mixture was added to each well when the cell density reached about 50%-70%. The RPMI-1640 medium with 10% FBS was replaced after transfection 6 h.

Proliferation of Jurkat cells by CCK-8 assay

The transfected cells in NC group and miR-146a mimic group were seeded into 96-well plate in the density of 2×10^3/well respectively, and each has three replicates. The CCK-8 was added at 24 h, 48 h, and 72 h, and then incubated at 37°C for 30 min. The absorbance of each well was measured at 490 nm wavelength and plotted the cell proliferation curves.

Cell cycle and apoptosis of Jurkat cells by flow cytometry

After transfection 24 h, 1×10^6 cells in each group were washed by pre-cooled PBS twice. Then Cell Cycle Assay Kit (BD, New Jersey, USA) was used to detect the cell cycle based on the protocol. Total 200 μl A solution was added to incubate at room temperature for 10 min, then 150 μl solution liquid was added to incubate at

room temperature for 10 min. Finally 120 μl C solution was incubated for 10 min in dark. Then flow cytometry was used and results were analyzed by Modfit software (Verity Software House Company, New York, USA). After transfection of AgomiR-146a 48 h, the collected cells were used to detect the apoptosis in different groups. The assay was used the ANXN V FITC APOPTOSIS DTEC KIT I (BD, New Jersey, USA) based on the standard protocol of manufactures, and the apoptosis was detected by Flow cytometry. Cells with positive ANNEXIN V were in early stage of apoptosis, and cells with positive PI were necrosis, while cells with the positive ANNEXIN V combined with positive PI were in late stage of apoptosis.

ShRNA interference of STAT1 expression in Jurkat cells

One day before transfection, 2×10^5 cells in logarithm growth were seeded into 24-well plate and cultured with antibiotic-free RPMI-1640 medium containing 10% FBS, which were divided into Normal control group, STAT1-shRNA transfection group, and negative control group. In the second day, the pGPU6/GFP/Neo-STAT1 shRNA plasmid was transfected based on the following procedure: 0.5 μl plasmid and 1 μl Lipo 2000 (Invitrogen, California, USA) was added into EP tubes containing 50 μl Opti Memi medium respectively. The 2 tubes were mixed together after 5 min standing, then followed by another 20 min standing at room temperature. The mixture was added to each well when the cell density reached about 70%-90%. The H-DMEM medium with 10% FBS was replaced after transfection 6 h. After culturing for another 48 h, GFP green fluorescent protein expression was observed under inverted fluorescence microscope, and flow cytometry was used to analyze transfection efficiency. Then the proliferation, cell cycle and apoptosis of cells transfected with STAT1-shRNA were detected by CCK-8 assay and flow cytometry as above.

Western blot analysis

After transfection 72 h, Jurkat cells were collected from normal control group, STAT1-shRNA interference group, and negative group to detect the protein changes of STAT1 by Western Blot. The collected cells were washed twice by precooled PBS, then lysed with RIPA to extract the total proteins. Mixed with 5× SDS loading buffer and boiled at 100°C for 10 min, the isolated proteins were separated by SDS-PAGE (60 v 30 min and 100 v 1 h) and then transferred to PVDF membrane (100 v 1 h). The primary antibody was rabbit anti-human STAT1 (1:1000) and mouse anti-human GAPDH antibody (1:10000) after blocking by 5% skim milk. The PVDF membrane was incubated overnight and washed by TBST for 5 times (each for 5 min). The second antibody was HRP-conjugated goat anti-rabbit (1:5000) and goat anti-mouse IgG (1:2000). All the antibodies were brought from the Bioworld Company (Minnesota, USA). Finally, the membrane was developed by enhanced ECL (Beyotime Biotechnology, Beijing, China). The inhibition ratio was calculated by the formula: (1-miRNA grey intensity/GAPDH grey intensity in miRNA group/grey intensity in control group/GAPDH grey intensity in blank group *100%).

Dual luciferase assay

Based on the bioinformatics prediction, the wild-type 3'UTR and the mutant 3'UTR of STAT1 were synthesized *in vitro* and were cloned into the downstream of pMIR-REPORT luciferase vector by Spe-1 and HindIII enzyme. And the mutant 3'UTR was regarded as control group. HEK293T cells were co-transfected with miR-146a mimics (100 nM) and wild-type STAT1 3'UTR or the mutant 3'UTR. After transfection for 24 h, cells were lysed and luciferase intensity was measured by GloMax 20/20 luminometer (Promega, Wisconsin, USA) based on the standard protocol of the luciferase kit (Beyotime Biotechnology, Beijing, China). The intensity of *Renilla* was used as control, and the fluorescence intensity in different groups was analyzed. All steps were followed the standard protocol of manufacture.

Statistical analysis

The SPSS 17.0 software was used to do statistical analysis. All the data were shown as the mean ± SD, and difference were determined by two-tailed Student's t-test. $P < 0.05$ was considered as statistically significant.

Results

MiR-146a expression in bone marrow and peripheral blood of children T-ALL

To investigate the roles of miR-146a in children T-ALL, qRT-PCR method was used to detect

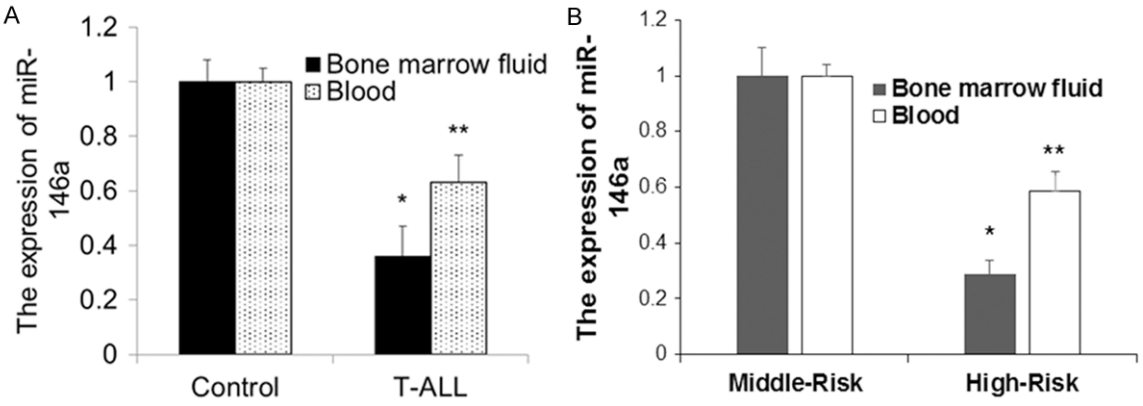

Figure 1. Expression of miR-146a in bone marrow and peripheral blood of children T-ALL. The expression of miR-181c was detected using qRT-PCR. A. miR-146a expression was decreased in T-ALL compared with control whether in bone marrow and peripheral blood ($P < 0.05$); B. miR-146a also decreased in high-risk group, compared with middle-risk group whether in bone marrow and peripheral blood ($P < 0.05$).

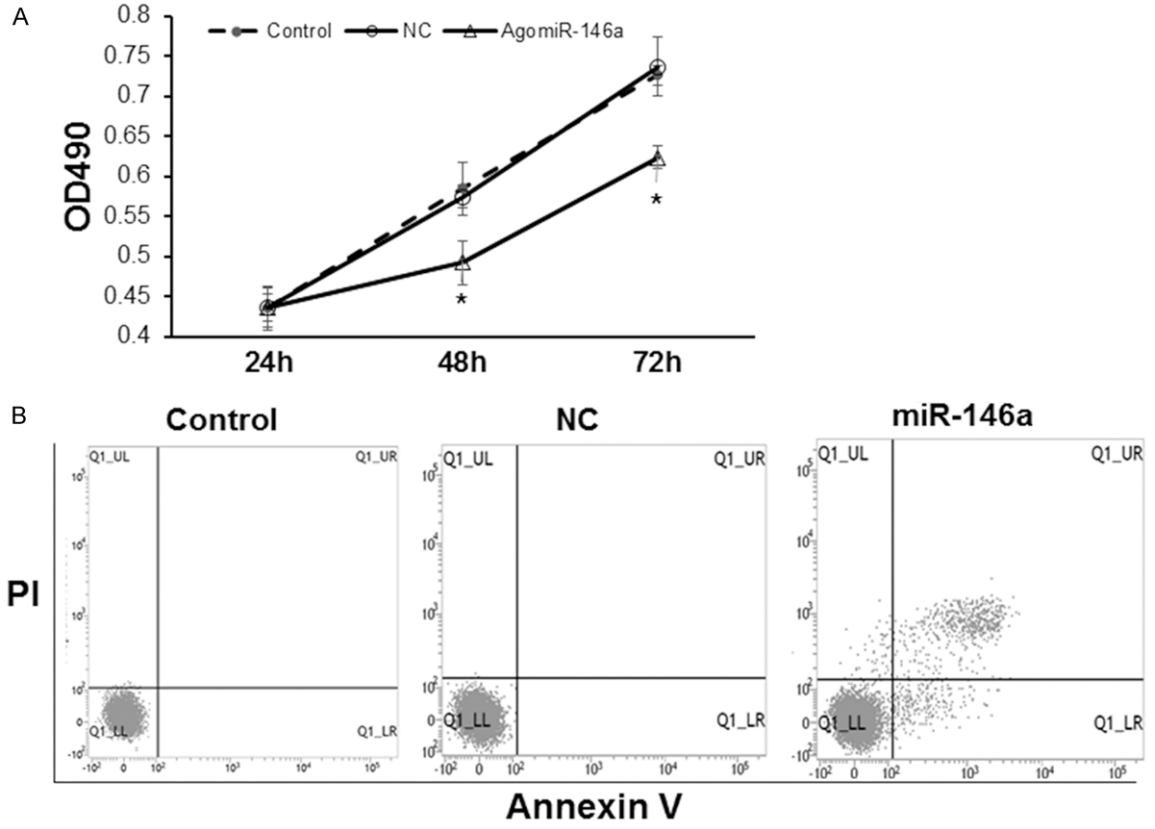

Figure 2. MiR-146a influences the proliferation and apoptosis of Jurkat cells. A. The proliferation of Jurkat cells was detected with CCK-8 assay; B. Flow cytometry analysis was used to detect the apoptosis of Jurkat cells.

expression changes of miR-146a. As shown in **Figure 1A**, it was shown that miR-146a was significantly decreased in bone marrow than in control group ($P < 0.05$). And miR-146a expression was significantly lower in high-risk group of children with T-ALL than in middle-risk group of children ($P < 0.05$) (**Figure 1B**). In peripheral blood, miR-146a expression had similar pattern with bone marrow. MiR-146a expression was higher in T-ALL children than in normal con-

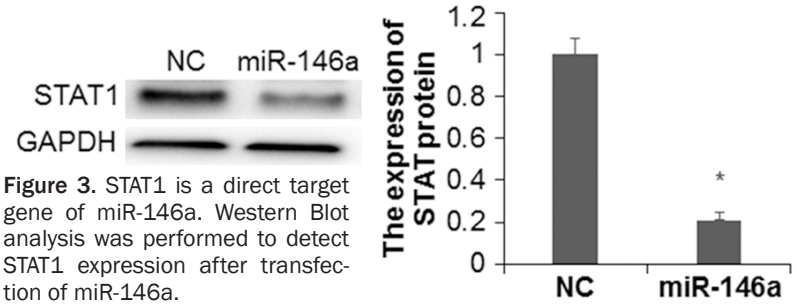

Figure 3. STAT1 is a direct target gene of miR-146a. Western Blot analysis was performed to detect STAT1 expression after transfection of miR-146a.

trol, and it was also significantly higher in high risk group than in risk group ($P < 0.05$). The results indicated that miR-146 may be associated with the development and progression of T-ALL.

Influence of miR-146a on proliferation and apoptosis of Jurkat cells

To study the effects of miR-146a on Jurkat proliferation and apoptosis, CCK-8 assay and flow cytometry were applied to detect the changes of Jurkat cells after transfection of miR-146a. Based on the CCK-8 assay, it was shown that proliferation rate of Jurkat cells was lower in AgomiR-146a group than in normal control group and negative control group (as shown in **Figure 2A**). And over-expressed miR-146a can significantly promote apoptosis of Jurkat cells ($P < 0.05$, as shown in **Figure 2B**). The results indicated that over-expressed miR-146a inhibited Jurkat proliferation and promoted apoptosis of Jurkat cells, which was consistent with the lower expression of miR-146a in children with T-ALL.

STAT1 expression by Western blot

Bioinformatics prediction indicated that STAT1 was one direct target gene of miR-146a. To validate whether miR-146a can regulate STAT1 expression, Western blot was used to detect the STAT1 protein expression. As shown in **Figure 3**, compared with the control group, STAT1 protein expression was significantly down-regulated in Jurkat cells with over-expressed miR-146a ($P < 0.05$). The results indicated that miR-146a can regulate STAT1 expression in Jurkat cells.

Influence on proliferation and apoptosis of Jurkat cells after STAT1 RNA interference

To investigate the roles of STAT1 in jurkat cells, we applied RNA interference technology to inhibit STAT1 expression, and then detected the changes of cell behaviors. After transfection of pGP-U6/GFP/Neo-STAT1 shRNA plasmid for 72 h by lipofection method, flow cytometry was used to detect the green fluorescence to estimate the transfection efficiency. It was shown that the transfection efficiency can reached about 37% (as shown in **Figure 4A**). The Western blot results showed that STAT1 expression was significantly decreased after RNA interference, which indicated that the effects of interference were good (**Figure 4B**). After interference, Jurkat cell proliferation was significantly decreased (**Figure 4C**), while apoptosis rate of Jurkat cells were increased (**Figure 4D**). All results indicated that the functions of down-regulated STAT1 were similar with roles of over-expressed miR-146a.

STAT1 is direct target gene of miR-146a

To determine whether STAT1 was targeted directly by miR-46a, we detected the GFP intensity by dual luciferase assay after co-transfection. As shown in **Figure 5**, fluorescence of cell lysis was significantly down-regulated in cells co-transfected with miR-146a mimics and pMIR-REPORT-STAT1 wild type plasmid than in control group ($P < 0.05$), while there was no significant difference between group co-transfected with miR-146a mimics and pMIR-REPORT-STAT1 mutant and group of normal control ($P > 0.05$). The results from dual luciferase assay indicated that miR-146a can regulate STAT1 expression through complementary bind to 3'-UTR.

Discussion

ALL is the most common pediatric malignancy disease, which has poor prognosis as it is less sensitive to chemotherapy, short remission and easy to relapse [13, 14]. In recent years, the remission rate of ALL has reached more than 90% as the deep understanding about the pathological mechanisms and improvement of chemotherapy, molecular targeted therapy, and stem cell transplantation technology. And the long-term disease-free survival has reached about 80%, while there is still about 20% of the

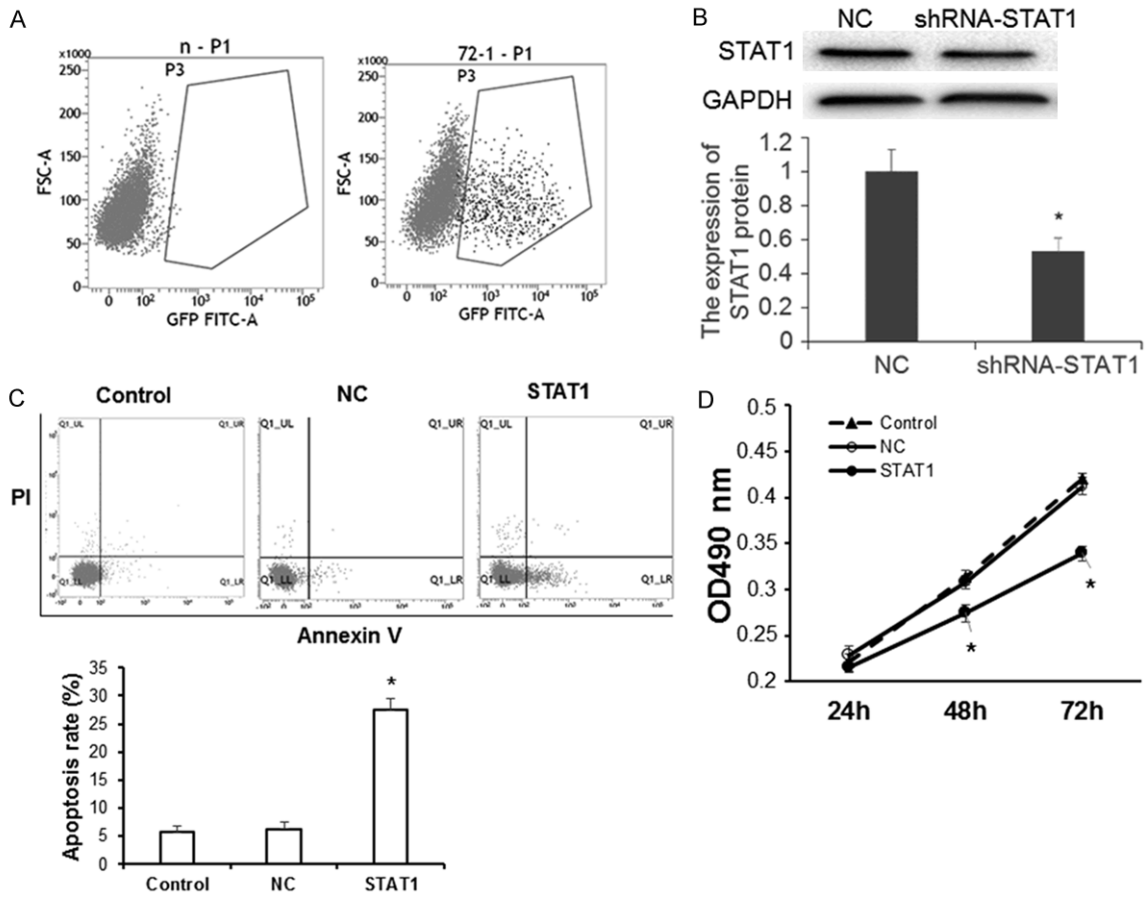

Figure 4. STAT1 influences the proliferation and apoptosis of Jurkat cells. A. Lipofection efficiency was detected by flow cytometry method; B. Western Blot was used to detect the expression of STAT1 in shRNA-STAR1 transfected cells; C. Flow cytometry analysis was used to detect the apoptosis of shRNA-STAR1 transfected Jurkat cells; D. The proliferation of shRNA-STAR1 transfected Jurkat cells was detected with CCK-8 assay.

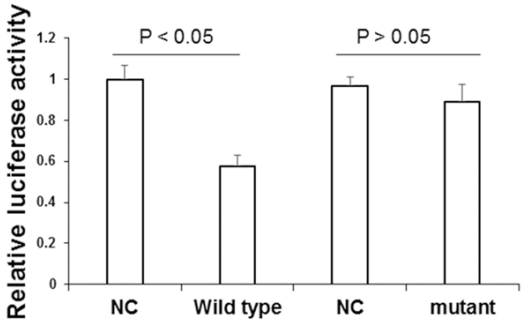

Figure 5. Dual luciferase assay was used to detect STAT1 is regulated by miR-146a.

children died of tumor recurrence [15]. Molecular targeted therapy has become the hot spot in clinic it is easily to relapse, poor prognosis, and the clinical and biological characteristics. MiR-146a is a class of small non-coding RNA molecules discovered recently. It was studied that miR-146a expression was increased in peripheral blood of non-small cell lung cancer, which can inhibit invasion and metastasis of non-small cell lung cancer [16]. Liu et al. found that Foxp3-miR-146a/NF-κB signaling pathway can inhibit apoptosis of breast cancer cells [17]. And over-expressed miR-146a can inhibit the invasion and metastasis of breast cancer cells [18]. These results indicated that miR-146a may play roles as tumor suppressor gene. In T-ALL of children patients, the mechanisms of how miR-146a participates into the development and progression of T-ALL are still unclear.

In this study, we examined miR-146 expression in bone marrow and peripheral blood of 54 children cases with T-ALL. The results showed that miR-146a expression was significantly decreased in bone marrow and peripheral blood of T-ALL children than in control group ($P < 0.05$).

And miR-146a expression was significantly lower in high risk group than in risk group ($P < 0.05$). The results indicated that down-regulated miR-146a was associated with the development of T-ALL. Jurkat cell line was from T cell lymphoma. Over-expressed miR-146a in Jurkat cells can repress the cell proliferation and promote the prognosis. It was predicted by bioinformatics tools that miR-146a can complementarily bind to 3'UTR of STAT1 mRNA. Western blot results indicated that STAT1 protein expression was significantly decreased after over-expression of miR-146a, which indicated that miR-146a may play roles by regulating STAT1 expression. So we applied RNA interference technology to down-regulate STAT1 expression. It was found that the proliferation of Jurkat cells was inhibited and the apoptosis was promoted after STAT1 down-regulation, which was consistent to the behavior changes of Jurkat cells when over-expressed miR-146a. Based on the results of dual luciferase assay, it can be concluded that miR-146a can inhibit Jurkat cell proliferation and promote apoptosis through complementarily binding to 3'UTR of STAT1 mRNA.

In summary, miR-146a expression was significantly decreased in bone marrow and peripheral blood in children patients with T-ALL. Through directly regulating STAT1 expression, miR-146a can inhibit cell proliferation and promote cell apoptosis of Jurkat cells in vitro. MiR-146a can be regarded as a potential treatment target for children with T-ALL, which has great clinical value.

Acknowledgements

The authors want to thank Ansheng Liu (Dean of Yan'an University Affiliated Hospital), Shiping Liu (Director of Yan'an University Affiliated Hospital) and Jihong Xue (from the Library of Yan'an University Affiliated Hospital) for their valuable helps to this work.

Disclosure of conflict of interest

None.

Address correspondence to: Kunxia Xie, Department of Pediatrics, Yan'an University Affiliated Hospital, No. 43, North Main Street, Baota District, Yan'an 716000, Shaanxi, China. Tel: 029-87297079; Fax: 029-87297079; E-mail: cxqc111@163.com

References

[1] Giambra V, Jenkins CE, Lam SH, Hoofd C, Belmonte M, Wang X, Gusscott S, Gracias D and Weng AP. Leukemia stem cells in T-ALL require active Hif1alpha and Wnt signaling. Blood 2015; 125: 3917-3927.

[2] Yokokawa Y, Taki T, Chinen Y, Kobayashi S, Nagoshi H, Akiyama M, Morimoto A, Ida H and Taniwaki M. Unique clonal relationship between T-cell acute lymphoblastic leukemia and subsequent Langerhans cell histiocytosis with TCR rearrangement and NOTCH1 mutation. Genes Chromosomes Cancer 2015; 54: 409-417.

[3] Silveira AB, Laranjeira AB, Rodrigues GO, Leal PC, Cardoso BA, Barata JT, Yunes RA, Zanchin NI, Brandalise SR and Yunes JA. PI3K inhibition synergizes with glucocorticoids but antagonizes with methotrexate in T-cell acute lymphoblastic leukemia. Oncotarget 2015; 6: 13105-13118.

[4] Nakano D, Ishitsuka K, Ikeda M, Tsuchihashi R, Okawa M, Okabe H, Tamura K and Kinjo J. Screening of promising chemotherapeutic candidates from plants against human adult T-cell leukemia/lymphoma (IV): phenanthroindolizidine alkaloids from Tylophora tanakae leaves. J Nat Med 2015; 69: 397-401.

[5] Ifuku H, Kusumoto S, Tanaka Y, Totani H, Ishida T, Okada M, Murakami S, Mizokami M, Ueda R and Iida S. Fatal reactivation of hepatitis B virus infection in a patient with adult T-cell leukemia-lymphoma receiving the anti-CC chemokine receptor 4 antibody mogamulizumab. Hepatol Res 2015; 45: 1363-7.

[6] Mishra AK, Duraisamy GS, Tycova A and Matousek J. Computational exploration of microRNAs from expressed sequence tags of Humulus lupulus, target predictions and expression analysis. Comput Biol Chem 2015; 59: 131-141.

[7] Baumgart BR, Gray KL, Woicke J, Bunch RT, Sanderson TP and Van Vleet TR. MicroRNA as biomarkers of mitochondrial toxicity. Toxicol Appl Pharmacol 2015; [Epub ahead of print].

[8] Wozniak MB, Scelo G, Muller DC, Mukeria A, Zaridze D and Brennan P. Circulating MicroRNAs as Non-Invasive Biomarkers for Early Detection of Non-Small-Cell Lung Cancer. PLoS One 2015; 10: e0125026.

[9] Wang T, Liu Y, Yuan W, Zhang L, Zhang Y, Wang Z, Zhou X, Zhou H, Chu T, Hao Y, Liu B, Zhao X, Lu L, Feng S and Kong X. Identification of microRNAome in rat bladder reveals miR-1949 as a potential inducer of bladder cancer following spinal cord injury. Mol Med Rep 2015; 12: 2849-2857.

[10] Frezzetti D, De Menna M, Zoppoli P, Guerra C, Ferraro A, Bello AM, De Luca P, Calabrese C, Fusco A, Ceccarelli M, Zollo M, Barbacid M, Di Lauro R and De Vita G. Upregulation of miR-21 by Ras in vivo and its role in tumor growth. Oncogene 2011; 30: 275-286.

[11] Tavazoie SF, Alarcón C, Oskarsson T, Padua D, Wang Q, Bos PD, Gerald WL and Massagué J. Endogenous human microRNAs that suppress breast cancer metastasis. Nature 2008; 451: 147-152.

[12] Turner M, Adhikari S and Subramanian S. Optimizing stem-loop qPCR assays through multiplexed cDNA synthesis of U6 and miRNAs. Plant Signal Behav 2013; 8.

[13] Losdyck E, Hornakova T, Springuel L, Degryse S, Gielen O, Cools J, Constantinescu SN, Flex E, Tartaglia M, Renauld JC and Knoops L. Distinct acute lymphoblastic leukemia (ALL)-associated Janus Kinase 3 (JAK3) mutants exhibit different cytokine-receptor requirements and JAK-inhibitor specificities. J Biol Chem 2015; 290: 29022-34.

[14] Liu S, Wei X, Mi R, Ai H, Yin Q, Wang P, Wang X, Fan R, Hu J, Zhu X, Zhou J, Fu Y and Song Y. Clinical features and survival analysis of patients with CD56 expression in de- novo acute myeloid leukemia with t8;21. Zhonghua Xue Ye Xue Za Zhi 2015; 36: 676-681.

[15] Kaszuba-Zwoinska J, Cwiklinska M, Balwierz W, Chorobik P, Nowak B, Wojcik-Piotrowicz K, Ziomber A, Malina-Novak K, Zaraska W and Thor PJ. Changes in cell death of peripheral blood lymphocytes isolated from children with acute lymphoblastic leukemia upon stimulation with 7 Hz, 30 mT pulsed electromagnetic field. Cell Mol Biol Lett 2015; 20: 130-142.

[16] Wang RJ, Zheng YH, Wang P and Zhang JZ. Serum miR-125a-5p, miR-145 and miR-146a as diagnostic biomarkers in non-small cell lung cancer. Int J Clin Exp Pathol 2015; 8: 765-771.

[17] Liu R, Liu C, Chen D, Yang WH, Liu X, Liu CG, Dugas CM, Tang F, Zheng P, Liu Y and Wang L. FOXP3 Controls an miR-146/NF-kappaB Negative Feedback Loop That Inhibits Apoptosis in Breast Cancer Cells. Cancer Res 2015; 75: 1703-1713.

[18] Tao SF, He HF and Chen Q. Quercetin inhibits proliferation and invasion acts by up-regulating miR-146a in human breast cancer cells. Mol Cell Biochem 2015; 402: 93-100.